



OPEN

The effect of cinnamon bark oil in bilateral common carotid artery occlusion-induced cerebral ischemia model in rats

Melike Aba ¹, Yuksel Kablanc ¹, Onural Ozhan ²✉, Elif Karaca ³, Ahmet Ulu ⁴, Burhan Ates ⁴, Nigar Vardi ³ & Hakan Parlakpinar ²

This study aimed to evaluate the protective and therapeutic effects of Cinnamon Bark Oil (CBO) on cerebral ischemia/reperfusion (I/R) injury in rats. The focus was on its potential antioxidant, anti-inflammatory, and antiapoptotic properties. Forty-four female *Wistar albino* rats were divided into four groups: Sham + CBO group, I/R + Vehicle group, prophylactic (CBO + I/R) group and therapeutic (I/R + CBO) group. Bilateral common carotid artery occlusion was performed to induce ischemia, followed by reperfusion for 72 h. CBO (100 mg/kg) was administered orally. Biochemical, histopathological, and immunohistochemical analyses were conducted, measuring oxidative stress markers, inflammatory cytokines, and neuronal degeneration in the cerebral cortex and hippocampus. Histopathological analysis revealed that CBO significantly reduced neuronal degeneration in both the prophylactic and therapeutic groups. Biochemically, CBO increased superoxide dismutase (SOD) and total antioxidant capacity (TAC), while decreasing malondialdehyde (MDA) and tumor necrosis factor-alpha (TNF- α) levels. Immunohistochemical staining showed decreased apoptotic markers (caspase-3, Bax) in the prophylactic and therapeutic groups. CBO demonstrated neuroprotective effects in cerebral I/R injury through its antioxidant, anti-inflammatory, and antiapoptotic properties. These findings suggest its potential as a complementary therapeutic agent for ischemic brain injuries.

Keywords Cerebral ischemia, Reperfusion injury, Cinnamon bark oil, Antioxidant, Anti-inflammatory, Anti-apoptotic

Abbreviations

ALT	Alanine aminotransferase
AST	Aspartate aminotransferase
Bcl-2	B-cell lymphoma 2
Bax	Bcl-2-associated protein x
BUN	Blood urea nitrogen
CBO	Cinnamon bark oil
CCAs	Common carotid arteries
CR	Creatinine
COX-2	Cyclooxygenase-2
H&E	Hematoxylin–eosin
HO-1	Heme oxygenase-1
H ₂ O ₂	Hydrogen peroxide
IHC	Immunohistochemical
iNOS	Inducible nitric oxide synthase
IL	Interleukin
I/R	Ischemia/reperfusion
MDA	Malondialdehyde

¹Department of Neurology, Faculty of Medicine, Inonu University, Malatya, Turkey. ²Department of Medical Pharmacology, Faculty of Medicine, Inonu University, 44280 Malatya, Turkey. ³Department of Histology and Embryology, Faculty of Medicine, Inonu University, Malatya, Turkey. ⁴Department of Biochemistry, Faculty of Arts and Sciences, Inonu University, Malatya, Turkey. ✉email: onural.ozhan@inonu.edu.tr

mmol eq trolox/L	Millimoles of trolox equivalents per liter
MPO	Myeloperoxidase
Nrf2	Nuclear factor erythroid 2-related factor 2
NF-κB	Nuclear factor-kappa B
OS	Oxidative stress
OSI	Oxidative stress index
PI3K	Phosphatidylinositol 3-kinase
AKT	Protein kinase B
SOD	Superoxide dismutase
TAC	Total antioxidant capacity
tGSH	Total glutathione
TOC	Total oxidant capacity
TNF	Tumor necrosis factor
U	Unit

Stroke is the second leading cause of death worldwide. Approximately 14 million people have stroke and approximately 5.5 million people die each year¹. Although it is a widespread disease with severe individual and social consequences, there is currently no treatment approach other than intravenous thrombolytic therapy and mechanical thrombectomy, which target reperfusion in the acute phase of ischemic stroke, are limited to a short time interval and can only be applied to patients who meet certain criteria². Recanalization provided by these treatments, which are considered the gold standard in acute stroke, does not always provide reperfusion in ischemic tissue or provides inadequate reperfusion, and sudden and rapidly increasing oxygen levels in brain tissue that has been in ischemia for a certain period of time cause functional, microscopic and sometimes macroscopic damage to the tissue with a series of reactions called oxygen paradox. This damage is added to the damage caused by ischemia and is called ischemia/reperfusion (I/R) damage³. This raises the issue of clinical trials and the development of other potential therapies in experimental animal models to prevent/reduce I/R injury that develops spontaneously in ischemic tissue in acute stroke or is induced by these recanalization therapies.

Ischemia-reperfusion injury triggers a multifaceted cascade of deleterious events. Reoxygenation after ischemia results in overproduction of reactive oxygen species (ROS), which overwhelms endogenous antioxidant defenses and leads to lipid peroxidation, protein oxidation, and DNA fragmentation. Concurrently, inflammatory pathways are activated, characterized by leukocyte infiltration, microglial activation, and the release of pro-inflammatory cytokines such as interleukin (IL)-1 β and tumor necrosis factor (TNF)- α , which amplify neuronal injury. Apoptosis also plays a pivotal role, as mitochondrial dysfunction and the upregulation of pro-apoptotic proteins [e.g., Bcl-2-associated protein x (Bax), caspase-3] coupled with downregulation of anti-apoptotic proteins [e.g., B-cell lymphoma 2 (Bcl-2)] shift the cellular balance toward programmed cell death. Collectively, these processes—oxidative stress (OS), inflammation, and apoptosis—contribute to neuronal loss and functional impairment following cerebral ischemia⁴⁻⁶.

Although there are more than 250 species of cinnamon plants distributed in different geographies in the world, Ceylon cinnamon and Chinese cinnamon are the two most important known species⁷⁻⁹. The *Cinnamomum zeylanicum* Blume (*Cinnamomum verum*) plant yields cinnamon essential oil. The most significant active ingredients in cinnamon are tannins, essential oil at a rate of 1–2%, benzaldehyde at a rate of 5–10%, eugenol and cinnamon at a rate of 60–70%¹⁰. *Trans*-cinnamaldehyde, an ingredient in cinnamon oil, possesses antioxidant and anti-inflammatory properties¹¹. Additionally, by preventing prostaglandin synthesis and cyclooxygenase activity, cinnamon bark oil (CBO) can reduce inflammation¹². In their 2007 study, Singh et al.¹³ documented the antioxidant activity of essential oils made from cinnamon leaves and bark. CBO and the eugenol component that was extracted from it were shown to have a potent antioxidant effect in the research conducted by Chericoni et al.¹⁴.

In order to comprehensively evaluate the potential of CBO, our experimental design incorporated both a prophylactic and a therapeutic group. The prophylactic group was intended to model preventive strategies that might be relevant in situations where ischemia is anticipated, such as in patients undergoing surgery with high cerebrovascular risk. In contrast, the therapeutic group was designed to mimic clinical scenarios in which treatment is initiated after ischemic injury has occurred, such as stroke or perioperative cerebral ischemia. Including both models allowed us to investigate whether CBO is more effective in preventing ischemic damage or in reducing injury after onset, thereby enhancing the translational value of our findings.

Therefore, the present study was designed to investigate the potential protective effects of *C. verum* against cerebral I/R injury in rats. Specifically, we aimed to evaluate whether CBO could attenuate OS, reduce inflammatory responses, and modulate apoptotic pathways, which are key pathological mechanisms in ischemic brain damage. By comparing these two approaches, we sought to determine not only whether CBO exerts neuroprotective effects, but also whether it is more effective as a preventive or therapeutic agent.

Materials and methods

Animals

In vivo tests were performed in accordance with the permission obtained from Inonu University Faculty of Medicine, Animal Experiments Local Ethics Committee (Ethical approval number: 2020/3-8). 44 rats 5 months old, healthy, female *Wistar albino* rats weighing between 228 and 333 g, which had not been used in any previous study, were used in the study. During the experiment, all rats were housed in conventional cages made of transparent plastic material at constant room temperature (22 ± 1 °C) and humidity ($60 \pm 5\%$) with 12:12 h light/dark cycle. Rats were fed ad libitum with 8 mm standard pellet feed offered over cage wires and fresh drinking

water daily in stainless steel ball drinkers. The experiments were completed in accordance with the ARRIVE guideline (Animal Experiments: Reporting of In Vivo Trials: ARRIVE Guideline) published in the British Journal of Pharmacology in 2010 to improve the quality and transparency of animal experimentation research¹⁵. The experimental part of the study was performed in the Laboratory of Inonu University Experimental Animal Production and Research Center using standard surgical instruments. All experimental procedures were performed according to the principles of care and use of laboratory animals.

Experimental design

The rats were simple randomly divided into four experimental groups:

Sham + CBO group (n=8): Only cervical incision was performed without carotid occlusion. Rats received 100 mg/kg CBO orally at 1, 24, 48, and 72 h.

I/R + Vehicle group (n=12): Rats were subjected to 15 min bilateral common carotid artery occlusion followed by 72 h reperfusion and received 1 mL sunflower oil (vehicle) orally at 1, 24, 48, and 72 h.

Prophylactic (CBO + I/R) group (n=12): Rats were pretreated with 100 mg/kg CBO orally at 72, 48, and 24 h before I/R, and an additional dose 1 h before occlusion, followed by 15 min ischemia and 72 h reperfusion.

Therapeutic (I/R + CBO) group (n=12): Rats were subjected to I/R and received 100 mg/kg CBO orally at 1, 24, 48, and 72 h after reperfusion.

The Sham + CBO group consisted of 8 rats, while the I/R groups consisted of 12 rats each, to account for greater variability and possible perioperative mortality. All animals survived in the Sham + CBO group (n=8), while survival was slightly lower in the ischemia–reperfusion groups due to perioperative mortality (I/R + Vehicle: n=8/12; Prophylactic CBO + I/R: n=8/12; Therapeutic I/R + CBO: n=8/12). All rats in each group (n=8) were included in body weight, brain weight, biochemical, and histopathological evaluations.

Two distinct treatment protocols were employed to explore different translational aspects. The prophylactic (CBO + I/R) group was included to evaluate the potential prophylactic use of CBO, modeling conditions where ischemia could be anticipated (such as perioperative settings). The post-treatment (I/R + CBO) group was designed to mimic a therapeutic intervention, in which CBO administration follows ischemic insult and reperfusion, thereby representing a clinically relevant treatment scenario for stroke or vascular surgery. This design enabled comparison of the prophylactic versus therapeutic efficacy of CBO.

Anesthesia procedure

All rats were fasted for 12 h prior to the study and ketamine hydrochloride (Ketasol 10% Richter Pharma AG, Wels, Austria; CAS no: 1867-66-9; 75 mg/kg) and xylazine hydrochloride (Xylazinbio 2% Bioveta A.S., Ivanovice na Hané, Czech Republic; CAS no: 23076-35-9; 10 mg/kg) mixture was anesthetized. Anesthesia of the rats was adjusted by controlling their paw withdrawal responses and to maintain spontaneous respiration during the experiment. Additional doses of ketamine hydrochloride were given intraperitoneal as needed to maintain anesthesia. An operation table with a rectal probe was used to maintain the body temperature of the rats between 36.5 and 37.5 °C during anesthesia.

Surgical procedure

After anesthesia was achieved, the rats were fixed on the operation table in supine position. After disinfecting the incision site with 10% povidone iodine, a skin incision was made in the midline of the pretracheal line and both common carotid arteries (CCAs) were carefully separated from the surrounding tissues and nervus vagus. In the experimental groups, CCAs were occluded bilaterally by using a separate atraumatic bulldog clamp for each artery from a single point and keeping the clamps closed simultaneously for 15 min, in accordance with previously described methods for global cerebral ischemia induction in rats^{16,17}. After this ischemia exposure, the clamps were released, the skin and subcutaneous tissue were closed with 3–0 silk suture, and the wound site was disinfected with 10% povidone iodine. Rats were reperfused for 72 h.

Rotarod/accelerod tests

Rotarod/Accelerod tests were performed on rats to measure motor activity, balance, and coordination. Rats were taught by repeatedly putting them on a revolving rod at the slowest speed (5 rpm) until they moved onto the rod on their own. After the rod stopped moving, the rats stayed there until the researcher removed them. Rotamex 4/8 system (Columbus Instruments International Corporation, Columbus, OH, USA) was used for both tests. In the rotarod test, the running time of the rats on the rotating shaft at constant speeds of 5, 10, 15, 20, 30, and 40 rpm (maximum 5 min) was determined. In the accelerod test, running on the accelerated spindle from 0 to 79 rpm in 4 min and 10 min was determined¹⁸.

Euthanasia procedure and tissue harvesting

Body weights of rats were measured individually at the beginning and end of the experiment using a calibrated digital scale. All experimental animals were euthanized by intraperitoneal injection of a mixture of high dose ketamine hydrochloride (225 mg/kg) and xylazine hydrochloride (30 mg/kg) at 72 h following ischemia. All rats were then subjected to thoracotomy procedure and intracardiac blood sampling was performed. Approximately 6–8 mL volume of blood was collected from all rats by entering the left ventricle. The blood samples were kept at room temperature for half an hour and then centrifuged at 2000 rpm for 10 min and the serum obtained were stored at –80 °C until analysis. For biochemical analyses, they were kept at room temperature for a while and then studied in the Central Laboratory of Inonu University Turgut Özal Medical Center. When blood collection was finished, bilateral fronto-parieto-occipital craniectomy was performed. The cerebrum, cerebellum and brain stem above the foramen magnum were completely removed without disrupting the anatomical integrity. Whole brains were carefully removed, rinsed with saline to remove blood residues, gently blotted dry on filter paper,

and weighed immediately using the same precision scale to determine brain weights. The right hemisphere was preserved at -80°C between aluminum foil for biochemical analysis. The left hemisphere was placed in 10% formaldehyde, subjected to routine tissue monitoring, embedded in paraffin and cut into 5μ thick sections for hematoxylin–eosin (H&E) staining and 3μ thick sections for immunohistochemical staining.

Cinnamon bark oil

CBO obtained by steam distillation from *Cinnamomum zeylanicum* Blume cinnamon bark (Sigma-Aldrich Missouri United States of America; CAS no: 8015-91-6) was obtained as a ready commercial product. The *C. zeylanicum* plant was transported in polyethylene bags and dried continuously at room temperature according to the manufacturer's instructions. CBO was produced by hydrodistillation technique. The plant material was roughly chopped and placed in a 2 L flask with 1.5 L of double distilled water. The mixture was boiled for 4 h. To extract the essential oil, the extract was concentrated in cooling steam. Sodium sulfate in anhydrous solution was used to dry the recovered oil. CBO was stored at 4°C before use.

C. verum was specifically chosen because it is widely recognized as the authentic “true cinnamon” and has a standardized phytochemical profile defined by the European Pharmacopoeia, with high cinnamaldehyde (55–75%) and low coumarin (<0.5%) content¹⁰. This makes it safer compared to other cinnamon species such as *C. cassia* or *C. burmannii*, which may contain higher coumarin levels¹⁹. Moreover, *C. verum* has been frequently used in experimental models investigating OS and inflammation, providing both safety and translational relevance^{20,21}.

For CBO administration, the rats were weighed separately and the amount of CBO to be administered for each rat was calculated at a dose of 100 mg/kg. The CBO dose and route of administration were chosen in accordance with the previous study of Ozhan et al., who demonstrated protective effects of 100 mg/kg oral CBO in rats without signs of toxicity. Therefore, 100 mg/kg was adopted in the present study to provide consistency with existing literature¹⁸. The CBO amounts calculated according to the body weight of the rats were weighed in an eppendorf tube on a precision balance and dissolved in sunflower oil used as vehicle solution in a volume of 1 mL. The Eppendorf tubes were vortexed to obtain a homogeneous mixture of CBO and sunflower oil. Then, sunflower oil containing CBO was administered orally to rats in a volume of 1 mL using a special orogastric cannula. Drug administration was performed at the same time every day to ensure equal dose intervals.

Biochemical analyzes

Serum biochemical analyzes

Blood urea nitrogen (BUN), creatinine (CR), albumin, aspartate aminotransferase (AST) and alanine aminotransferase (ALT) levels were determined in the Central Laboratory of Turgut Özal Medical Center to evaluate solid organ damage.

Brain tissue biochemical analyzes

Weighed 100 mg of brain tissue was taken into plastic tubes and 1 mL of phosphate buffered saline (pH 7.4) was added. The weighed tissue samples were homogenized with a homogenizer under ice isolation until the tissue samples were completely disintegrated. The homogenates obtained were then sonified 4 times for 15 s at 30 s intervals with a sonifier, again under ice isolation. After sonification, the homogenates were centrifuged at 14,000 rpm for 15 min at $+4^{\circ}\text{C}$ using a refrigerated centrifuge. Finally, the obtained supernatants were stored at $+4^{\circ}\text{C}$ until the measurement procedures were performed. For biochemical analyses, malondialdehyde (MDA), superoxide dismutase (SOD), and total glutathione (tGSH) levels were measured by spectrophotometer from the homogenate of tissue samples. Total oxidant capacity (TOC), total antioxidant capacity (TAC), and oxidative stress index (OSI) were also evaluated in brain tissue. Myeloperoxidase (MPO), TNF- α , and IL-1 levels were measured to evaluate the inflammatory response in brain tissue.

Total protein determination

Total protein concentration in the samples was determined by the Bradford method, which is a fast and simple method²². Bradford reagent was added to the homogenate samples and the total protein amount was determined by measuring the absorbance change at 595 nm. Bovine serum albumin was used as standard protein. Total protein concentration was used as a normalization factor in the evaluation of the specific activities of the biochemical parameters studied.

Tissue superoxide dismutase activity measurement

SOD enzyme activity in tissues was measured according to the method previously described by McCord and Fridovich in the literature²³. Basis of the method: SOD enzyme activity inhibits the reduction of cytochrome-c by superoxide radicals produced by xanthine/xanthine oxidase system. In this method, SOD enzyme activity is based on measuring this inhibition. The amount of SOD inhibiting this reaction by 50% was considered as 1 unit (U). SOD enzyme activity was measured by following kinetics at 550 nm and the results were given as U/mg protein.

Tissue total glutathione measurement

tGSH in tissues was measured using the method described by Akerboom and Sies²⁴. Basis of the method: This method is based on the spectrophotometric measurement at 412 nm of the increase in the compound 5-thio-2-nitrobenzoate formed by the reaction of 5,5'-dithio-bis(2-nitrobenzoic acid), nicotinamide adenine dinucleotide phosphate and glutathione reductase. The absorbance change was monitored in UV-vis spectrophotometer at 412 nm wavelength for 15 min. The results obtained were expressed in nmol/mg protein.

Malondialdehyde measurement

MDA measurement was performed using the method previously described by Placer et al.²⁵ in the literature. Basis of the method: It is based on the measurement of the pink colored product formed as a result of the reaction of MDA, the breakdown product of peroxidized lipids, with thiobarbituric acid at 532 nm. 1,1,3,3-tetraethoxypropane was used as a standard. MDA content of the samples was expressed as nmol/mg protein.

Myeloperoxidase activity measurement

For MPO activity measurement was performed using the method Pulli et al.²⁶. Tissue samples were weighed 0.1 g and homogenized under ice isolation. The samples were then centrifuged at 10.000 rpm for 15 min at +4°C to separate the pellets. The pellets were separated from the supernatant and added to 0.1% HETAB solution. The solutions were then sonified for 15 s, frozen at -80°C and then thawed again. This sonification-freezing-thawing procedure was performed 3 times in succession. The samples were then centrifuged at 10.000 rpm for 15 min to remove the supernatants and 25 µL of supernatant and 200 µL of o-dianisidine solution (pH:6) were added to 96-well plates. Absorbances were measured after 5 min at 460 nm wavelength using a microplate reader. MPO activity results were expressed as U/g wet tissue.

Total antioxidant capacity and total oxidant capacity measurement

TAC level in tissue homeostats was determined using a kit (Rel Assay Diagnostics kit, Mega Tip, Gaziantep, Türkiye) developed by Erel^{27,28}. With this method, hydroxyl radical is produced. The antioxidative effect of the sample against the hydroxyl radicals produced can be measured spectrophotometrically. Results were expressed as millimoles of trolox equivalents per liter (mmol eq trolox/L).

TOC level in tissue homeostats was determined using a kit (Rel Assay Diagnostics kit, Mega Tip, Gaziantep, Türkiye) developed by Erel²⁹. The basis of the method is as follows: Oxidants present in the sample oxidize the ferrous ion o-dianisidine complex to iron ion. The oxidation reaction is enhanced by the abundant glycerol molecules in the reaction medium. The ferric ion forms a colored complex with xylenol orange in an acidic medium. The absorbance, which can be measured spectrophotometrically, is directly proportional to the amount of oxidant molecules present in the sample. Hydrogen peroxide (H₂O₂) was used as a standard and results were expressed in micromoles H₂O₂ equivalent/L.

Oxidative stress index

To calculate OSI, the formula OSI = TOC (micromol H₂O₂ equivalent/L)/TAC (micromol trolox equivalent/L) was used.

Tumor necrosis and factor- α interleukin-1 measurement

TNF- α and IL-1 levels were measured using ELISA kits developed by Shanghai Sunred Biological Technology Co. Results were expressed in ng/L.

Histopathologic examination

Brain tissues were embedded in paraffin and serially sectioned. From each block, 5-µm sections were obtained for H&E staining and 3-µm sections for immunohistochemical staining. For each animal, 10 non-overlapping fields from both the cerebral cortex and hippocampus were analyzed. Although routine serial cutting was performed, representative sections were selected at regular intervals rather than every consecutive section. For histopathologic evaluation, the brain tissues of the rats were dissected into small 3–4 mm pieces. They were then placed in plastic tissue tracking cassettes and fixed in 10% formaldehyde for 24 h. After fixation, the brain tissue samples were placed in formaldehyde solution and tissue tracking procedure was performed on the Tissue-Tek VIP/SAKURA tissue tracking device. According to this procedure, tissue samples were washed in running tap water for 24 h, dehydrated in graded alcohols, cleared in xylene and embedded in paraffin blocks. 5 µm thick sections were prepared from the paraffin blocks using a Leica RM2145 microtome. The sections taken on slides were stained with H&E to observe the general histologic structure. In addition, Bax [(Bax (B-9) sc-7480 Santa Cruz Biotechnology CA, USA) and caspase-3 (Caspase 3 Ab-4; Neomarkers, Fremont, CA) immunohistochemical (IHC) staining procedure was performed to observe cells undergoing apoptosis. Degenerated neurons were evaluated in 10 different areas in the cerebral cortex and hippocampus using X40 objective. Photographs were obtained for all groups. Neurons with acidophilic cell cytoplasm, heterochromatic and shrunken nuclei were defined as degenerated. The number of caspase 3 (+) and Bax (+) cells was then calculated. Stained slides were analyzed using a Leica DFC280 light microscope and Leica Q Win Image Analysis System (Leica Microsystems Imaging Solution Ltd, Cambridge, UK).

Statistical analysis

Data were presented as mean \pm standard deviation and median (min–max). The conformity of quantitative data to normal distribution was analyzed by the Shapiro–Wilk test. Intergroup comparisons of normally distributed variables were performed by one-way ANOVA, whereas non-normally distributed variables were analyzed using the Kruskal–Wallis test. Specifically, brain weights and rotarod/accelerod performance tests were evaluated with the Kruskal–Wallis test, while all other biochemical, histopathological, and immunohistochemical parameters were assessed by one-way ANOVA. A 2 \times 4 repeated measures ANOVA was conducted with time (baseline vs. final) as the within-subjects factor and treatment group as the between-subjects factor for rat body weights. When significant overall differences were detected, appropriate post hoc tests (Tukey for ANOVA, Dunn's test with Bonferroni correction for Kruskal–Wallis) were applied for pairwise group comparisons. IBM SPSS

Groups (n=8)	Sham + CBO Group	I/R + Vehicle Group	CBO + I/R Group	I/R + CBO Group	p value
5 rpm (sec)	300 (122–300)	300 (82–300)	300 (300–300)	300 (63–300)	0.270
10 rpm (sec)	300 (24–300)	300 (50–300)	300 (213–300)	300 (75–300)	0.562
15 rpm (sec)	300 (72–300)	221 (34–300)	141 (43–300)	99 (43–300)	0.420
20 rpm (sec)	56 (15–300)	51 (26–158)	40 (12–144)	38 (16–74)	0.544
30 rpm (sec)	19 (6–300)	34 (12–103)	22 (3–83)	17 (0–58)	0.940
40 rpm (sec)	11 (2–22)	13 (2–71)	8 (2–86)	5 (0–64)	0.619
0–79 rpm 4 min (sec)	84 (57–120)	81 (51–122)	89 (59–141)	75 (48–181)	0.642
0–79 rpm 10 min (sec)	184 (105–220)	187 (52–220)	175 (128–239)	151 (133–341)	0.709

Table 1. Results of rotarod and accelerod performance tests in the study groups (Sham + CBO, I/R + vehicle, CBO + I/R, and I/R + CBO). Values are expressed as median (min–max). Reported p-values represent overall group differences obtained by Kruskal–Wallis test. No statistically significant differences were found between the groups ($p > 0.05$).

Group	Baseline (g)*	Final (g)*	Change (g)*	ANOVA results
Sham + CBO	280.63 ± 36.87	269.88 ± 33.42	-10.75 ± 36.87	
I/R + Vehicle	257.22 ± 32.85	245.11 ± 45.23	-12.11 ± 51.27	
CBO + I/R	257.45 ± 24.67	248.27 ± 26.89	-9.18 ± 31.96	
I/R + CBO	262.00 ± 28.94	250.63 ± 29.87	-11.38 ± 40.04	
Statistical Effects				<i>F (df) p-value</i>
Between Groups				2.704 (3,32) 0.061
Time				1.482 (1,36) 0.231
Group × Time				0.011 (3,36) 0.998

Table 2. Body weight of rats at baseline and after the experimental procedures across the study groups (Sham + CBO, I/R + vehicle, CBO + I/R, and I/R + CBO). Reported p-values represent overall group differences obtained by repeated measures ANOVA (time, group, and group × time interaction). CBO, Cinnamon Bark Oil; I/R, Ischemia–Reperfusion. *Data presented as mean ± standard deviation.

Statistics 22.0 (IBM Corp., Armonk, NY, USA) was used for all statistical analyses, and values of $p < 0.05$ were considered statistically significant.

Results

Although 12 rats were initially allocated to each I/R group, perioperative mortality occurred in four animals per group. Therefore, the analyses were conducted with the remaining 8 rats in each I/R subgroup, whereas all 8 rats survived in the Sham + CBO group.

Rotarod/accelerod tests

In both the rotarod and accelerod tests, no statistically significant differences were observed between the experimental groups ($p > 0.05$) (Table 1).

Rat body and brain weights

The analysis revealed no significant main effect of group ($F_{3,32} = 2.704, p = 0.061$), no significant main effect of time ($F_{1,36} = 1.482, p = 0.231$), and no significant group × time interaction ($F_{3,36} = 0.011, p = 0.998$). The extremely high p-value for the interaction term ($p = 0.998$) indicates that all treatment groups exhibited nearly identical weight change patterns over time. These findings demonstrate that neither the treatment interventions nor the temporal factor significantly influenced body weight changes, and there were no differential treatment effects across the experimental period.

There was no statistically significant difference between the groups in terms of brain weight ($p > 0.05$). The findings are summarized in Tables 2 and 3.

Biochemical findings

Serum biochemical findings

BUN, CR, albumin, AST, and ALT levels were compared in blood samples obtained from all rats in the groups before sacrifice to evaluate solid organ damage. No statistically significant difference was found between the groups in the comparison of serum BUN, CR, albumin, AST, and ALT levels ($p > 0.05$). The findings are shown in Fig. 1.

Groups	Brain weight (g)
Sham + CBO (n=8)	1.96 (1.62–2.23)
I/R + Vehicle (n=8)	2.00 (1.80–2.28)
CBO + I/R (n=8)	2.11 (1.94–2.63)
CBO + I/R (n=8)	2.04 (1.86–2.21)

Table 3. Comparison of brain weight among the study groups (Sham + CBO, I/R + Vehicle, CBO + I/R, and I/R + CBO). Values are expressed as median (min–max). Reported p-values represent overall group differences obtained by Kruskal–Wallis test. CBO, Cinnamon Bark Oil; I/R, Ischemia–Reperfusion.

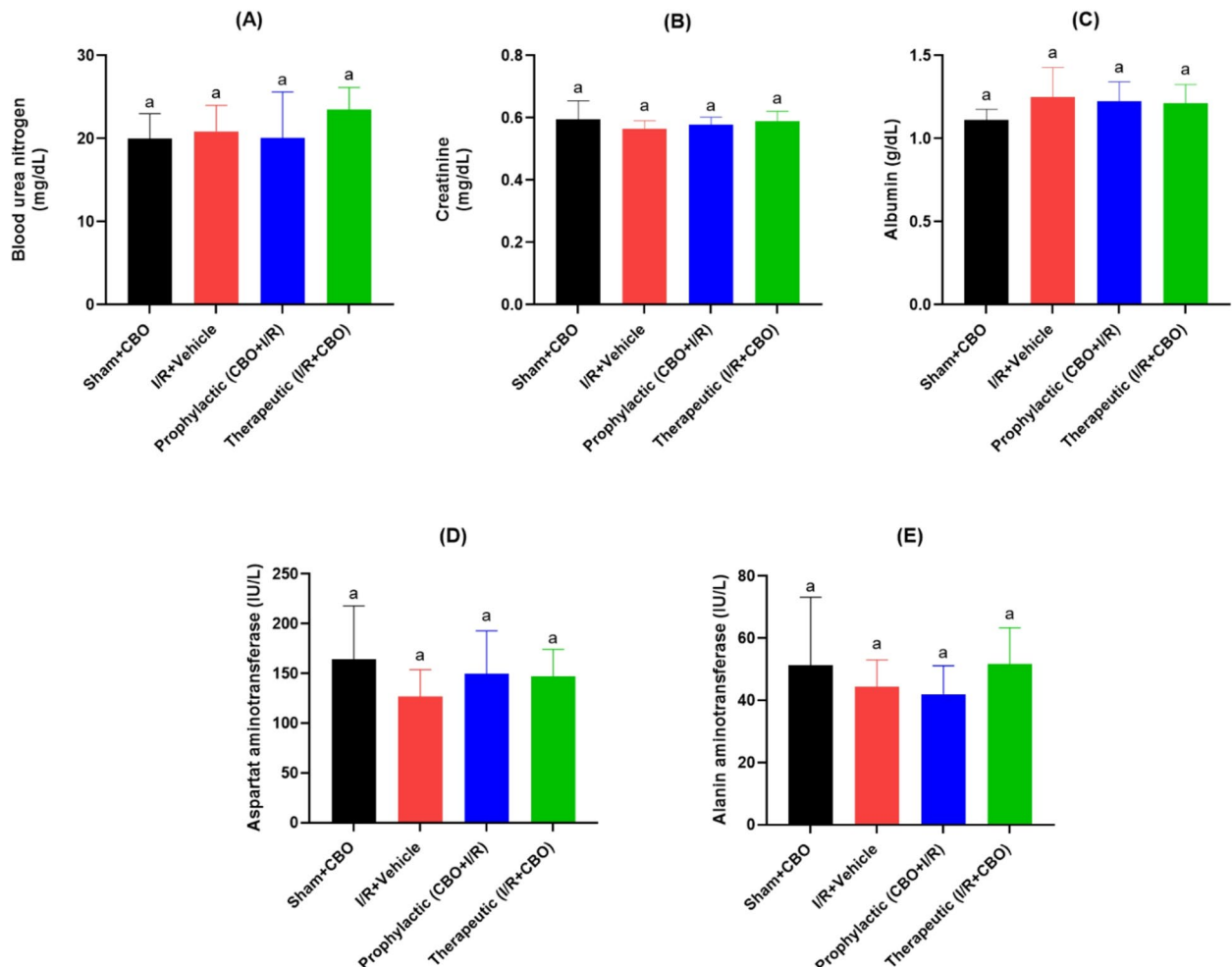


Fig. 1. Serum biochemical findings. (A) Blood urea nitrogen levels; (B) Creatinine levels; (C) Albumin levels; (D) Aspartate aminotransferase levels; and (E) Alanine aminotransferase levels. CBO: Cinnamon Bark Oil; and I/R: Ischemia–Reperfusion. Values are represented as mean \pm SD (n=8). Different letters indicate statistical significance using one-way ANOVA followed by Tukey's multiple comparison tests.

Malondialdehyde levels

There was a statistically significant difference in MDA levels between Sham + CBO and CBO + I/R, CBO + I/R and I/R + Vehicle, I/R + CBO and I/R + Vehicle, Sham + CBO and I/R + CBO, CBO + I/R and I/R + CBO groups ($p < 0.05$).

While the mean MDA levels of the Sham + CBO and I/R + Vehicle groups were similar ($p > 0.05$), the MDA level in the CBO + I/R group was lower than the MDA level in the Sham + CBO group and this difference was statistically significant ($p < 0.05$). The MDA level in the I/R + CBO group was lower than the MDA level in the Sham + CBO group and this difference was statistically significant ($p < 0.05$). The MDA level in the I/R + CBO group was lower than the MDA level in the CBO + I/R group and this difference was statistically significant ($p < 0.05$). The MDA level in the CBO + I/R group was lower than the MDA level in the I/R + Vehicle group and

this difference was found to be statistically significant ($p < 0.05$). The MDA level in the I/R + CBO group was significantly lower than the MDA level in the I/R group ($p < 0.05$).

The findings are shown in Fig. 2A.

Superoxide dismutase enzyme activity levels

Sham + CBO and CBO + I/R, I/R + Vehicle and CBO + I/R groups were found to be significantly different in terms of SOD levels ($p < 0.05$).

The SOD level in the CBO + I/R group was higher than the SOD level in the Sham + CBO group and this difference was statistically significant ($p < 0.05$). The SOD level in the CBO + I/R group was significantly higher than the SOD level in the I/R + Vehicle group ($p < 0.05$). On the other hand, there was no statistically significant difference in SOD levels between I/R + CBO and Sham + CBO, I/R + CBO and I/R + Vehicle, I/R + CBO and CBO + I/R groups ($p > 0.05$).

The findings are shown in Fig. 2B.

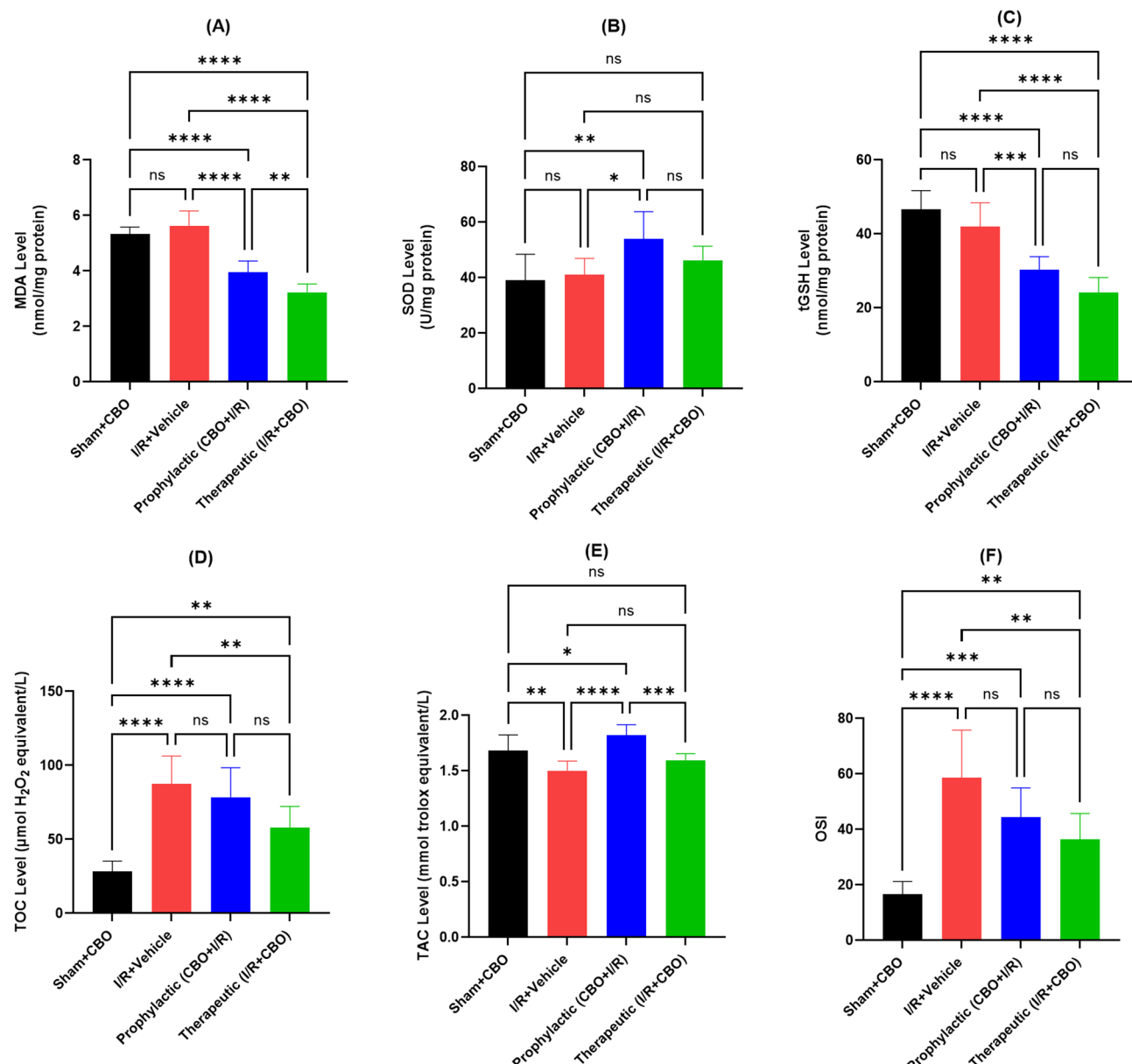


Fig. 2. Biochemical analyses in brain tissue. (A) MDA levels; (B) SOD levels; (C) tGSH levels; (D) TOC levels; (E) TAC levels; and (F) OSI values. CBO: Cinnamon Bark Oil; and I/R: Ischemia–Reperfusion. Values are represented as mean \pm SD ($n = 8$). Asterisks indicate statistical significance using one-way ANOVA followed by Tukey's multiple comparison tests. * $p < 0.05$, ** $p < 0.01$, *** $p < 0.001$, **** $p < 0.0001$, and ns, not statistically significant.

Total glutathione levels

Sham + CBO and CBO + I/R, Sham + CBO and I/R + CBO, I/R + Vehicle and CBO + I/R, I/R + Vehicle and I/R + CBO, CBO + I/R and I/R + CBO groups were significantly different in terms of tGSH levels ($p < 0.05$).

The tGSH level in the Sham + CBO group was significantly higher than the tGSH level in the CBO + I/R group ($p < 0.05$). The tGSH level in the Sham + CBO group was higher than the tGSH level in the I/R + CBO group and this difference was found to be significant ($p < 0.05$). The tGSH level in the I/R + Vehicle group was significantly higher than the tGSH level in the CBO + I/R group ($p < 0.05$). The tGSH level in the I/R + Vehicle group was higher than the tGSH level in the I/R + CBO group and the tGSH level in the CBO + I/R group was higher than the tGSH level in the I/R + CBO group and this difference was statistically significant ($p < 0.05$). In contrast, there was no statistically significant difference in tGSH levels between Sham + CBO and I/R + Vehicle, I/R + CBO and CBO + I/R groups ($p > 0.05$).

The findings are shown in Fig. 2C.

Total oxidant capacity

There was a statistically significant difference in TOC levels between Sham + CBO and I/R + Vehicle, Sham + CBO and CBO + I/R, Sham + CBO and I/R + CBO, CBO + I/R and I/R + CBO groups ($p < 0.05$).

TOC level in I/R + Vehicle group was higher than that in Sham + CBO group, TOC level in CBO + I/R group was higher than that in Sham + CBO group, TOC level in I/R + CBO group was higher than that in Sham + CBO group and this difference was statistically significant ($p < 0.05$). TOC level in I/R + CBO group was lower than that in CBO + I/R group and this difference was statistically significant ($p < 0.05$). There was no statistically significant difference in TOC levels between CBO + I/R and I/R + Vehicle, I/R + CBO and I/R + Vehicle groups ($p > 0.05$).

The findings are shown in Fig. 2D.

Total antioxidant capacity

Sham + CBO and CBO + I/R, I/R + Vehicle and CBO + I/R, I/R + Vehicle and I/R + CBO, CBO + I/R and I/R + CBO groups were significantly different from each other in terms of TAC levels ($p < 0.05$).

The TAC level in the CBO + I/R group was higher than the TAC level in the Sham + CBO group, the TAC level in the CBO + I/R group was higher than the TAC level in the I/R + Vehicle group and the TAC level in the I/R + CBO group was higher than the TAC level in the I/R + Vehicle group and this difference was found to be statistically significant ($p < 0.05$). In addition, the TAC level in the CBO + I/R group was significantly higher than the TAC level in the I/R + CBO group ($p < 0.05$). In contrast, there was no statistically significant difference in TAC levels between Sham + CBO and I/R + CBO, I/R + Vehicle and I/R + CBO groups ($p > 0.05$).

The findings are shown in Fig. 2E.

Oxidative stress index

There was a statistically significant difference in OSI values between Sham + CBO and I/R + Vehicle, Sham + CBO and CBO + I/R, Sham + CBO and I/R + CBO, I/R + Vehicle and I/R + CBO groups ($p < 0.05$).

The OSI value in the I/R + Vehicle group was higher than the OSI value in the Sham + CBO group, the OSI value in the CBO + I/R group was higher than the OSI value in the Sham + CBO group and the OSI value in the I/R + CBO group was higher than the OSI value in the Sham + CBO group and this increase was statistically significant ($p < 0.05$). The OSI value in the I/R + CBO group was statistically significantly lower than the OSI value in the I/R + Vehicle group ($p < 0.05$). On the other hand, there was no statistically significant difference in OSI values between CBO + I/R and I/R + Vehicle, I/R + CBO and CBO + I/R groups ($p > 0.05$).

The findings are shown in Fig. 2F.

Myeloperoxidase enzyme levels

There was a statistically significant difference in MPO levels between Sham + CBO and CBO + I/R, Sham + CBO, and I/R + CBO groups ($p < 0.05$).

The MPO level in the CBO + I/R group was higher than the MPO level in the Sham + CBO group and the MPO level in the I/R + CBO group was higher than the MPO level in the Sham + CBO group and this difference was statistically significant ($p < 0.05$). However, there was no statistically significant difference in MPO levels between I/R + CBO and I/R + Vehicle, CBO + I/R and I/R + Vehicle, I/R + CBO and CBO + I/R groups ($p > 0.05$).

The findings are shown in Fig. 3A.

Tumor necrosis factor- α levels

There was a statistically significant difference in TNF- α levels between Sham + CBO and I/R + Vehicle, I/R + Vehicle and CBO + I/R, I/R + Vehicle and I/R + CBO groups ($p < 0.05$).

TNF- α level in the I/R + Vehicle group was higher than the TNF- α level in the Sham + CBO group, TNF- α level in the I/R + Vehicle group was higher than the TNF- α level in the CBO + I/R group and TNF- α level in the I/R + Vehicle group was higher than the TNF- α level in the I/R + CBO group and this difference was statistically significant ($p < 0.05$).

On the other hand, there was no statistically significant difference in TNF- α levels between CBO + I/R and Sham + CBO, I/R + CBO and Sham + CBO, I/R + CBO and CBO + I/R groups ($p > 0.05$).

The findings are shown in Fig. 3B.

Interleukin-1 levels

When the groups were compared in terms of IL-1 levels, no statistically significant difference was found ($p > 0.05$).

The findings are shown in Fig. 3C.

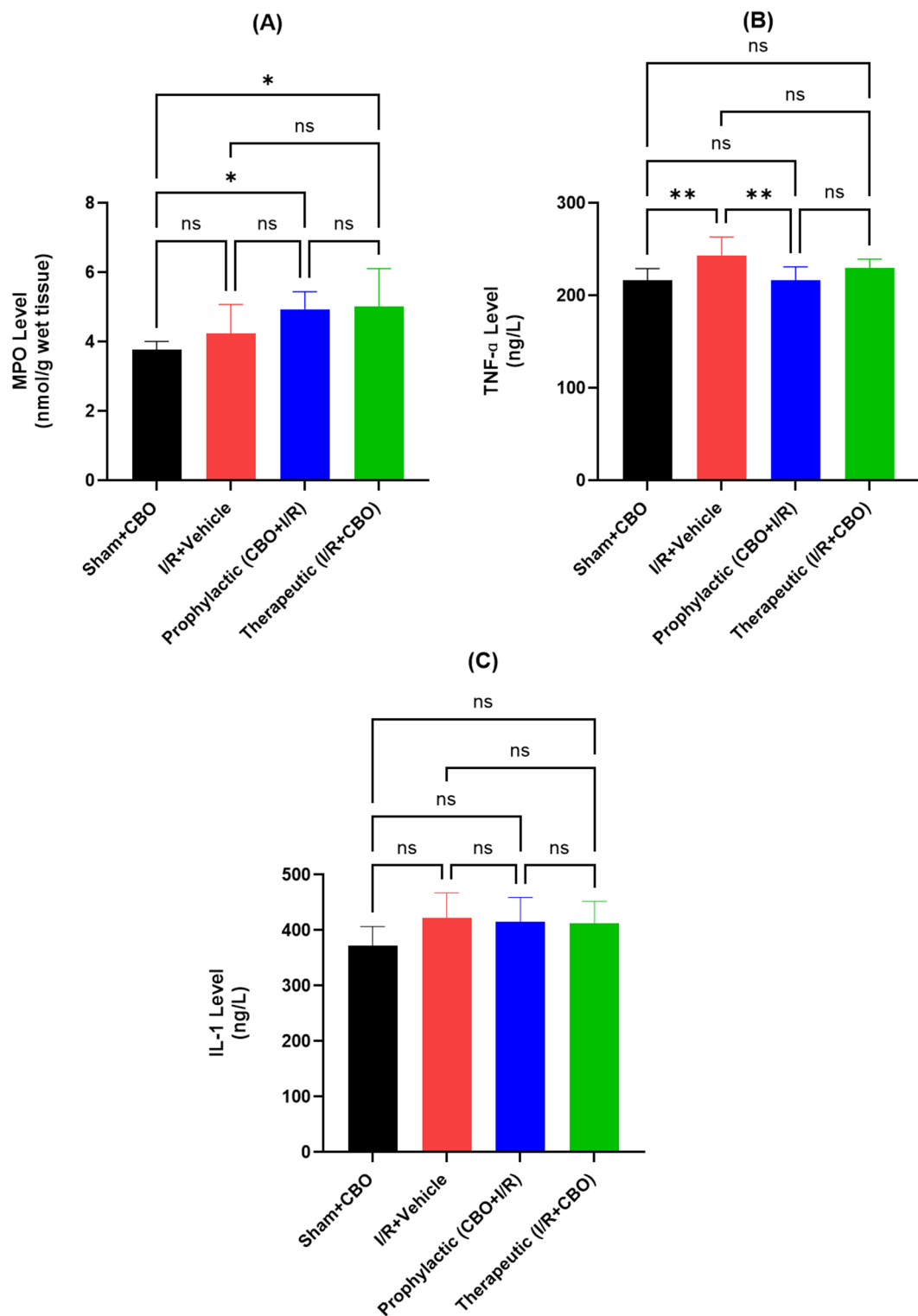


Fig. 3. Comparison of inflammatory parameters for brain tissue. (A) MPO levels; (B) TNF- α levels; and (C) IL-1 levels. CBO, Cinnamon Bark Oil; I/R, Ischemia–Reperfusion. Values are represented as mean \pm SD (n = 8). Asterisks indicate statistical significance using one-way ANOVA followed by Tukey's multiple comparison tests. * $p < 0.05$, ** $p < 0.01$, and ns, not statistically significant.

Histopathologic findings

In the Sham + CBO group, normal histologic structure of the cortex and hippocampus region of the brain tissue was observed in the H&E stained sections (Figs. 4 and 5).

I/R + Vehicle group: H&E stained sections showed degenerated neurons with irregular borders, acidophilic cytoplasm and increased nucleus density in the cerebral cortex and hippocampus. The number of degenerated neurons in this group was 6.24 ± 0.22 in the cortex and 6.28 ± 2.45 in the hippocampus. When compared with the Sham + CBO group, the number of degenerated neurons in the cortex and hippocampus regions was found to be statistically significantly increased ($p < 0.0001$). The number of caspase-3 (+) cells was 7.04 ± 2.04 in the cortex and 3.60 ± 1.33 in the hippocampus in the sections where caspase-3 staining method was applied. Compared to the Sham + CBO group, the number of caspase-3 (+) cells in this group was statistically significantly increased ($p < 0.0001$). The number of Bax (+) cells in the Bax staining method was found to be 9.67 ± 2.95 in the cortex and 11.95 ± 3.75 in the hippocampus. When compared with the Sham + CBO group, the number of Bax (+) cells in this group was found to be statistically significantly increased ($p < 0.0001$) (Figs. 4 and 5; Table 4).

Prophylactic (CBO + I/R) group: The number of degenerated neurons in H&E stained sections was 3.84 ± 1.66 in the cortex and 2.21 ± 1.16 in the hippocampus in this group. Compared to the I/R + Vehicle group, the number of degenerated neurons in the cortex and hippocampus regions was statistically significantly decreased ($p < 0.0001$).

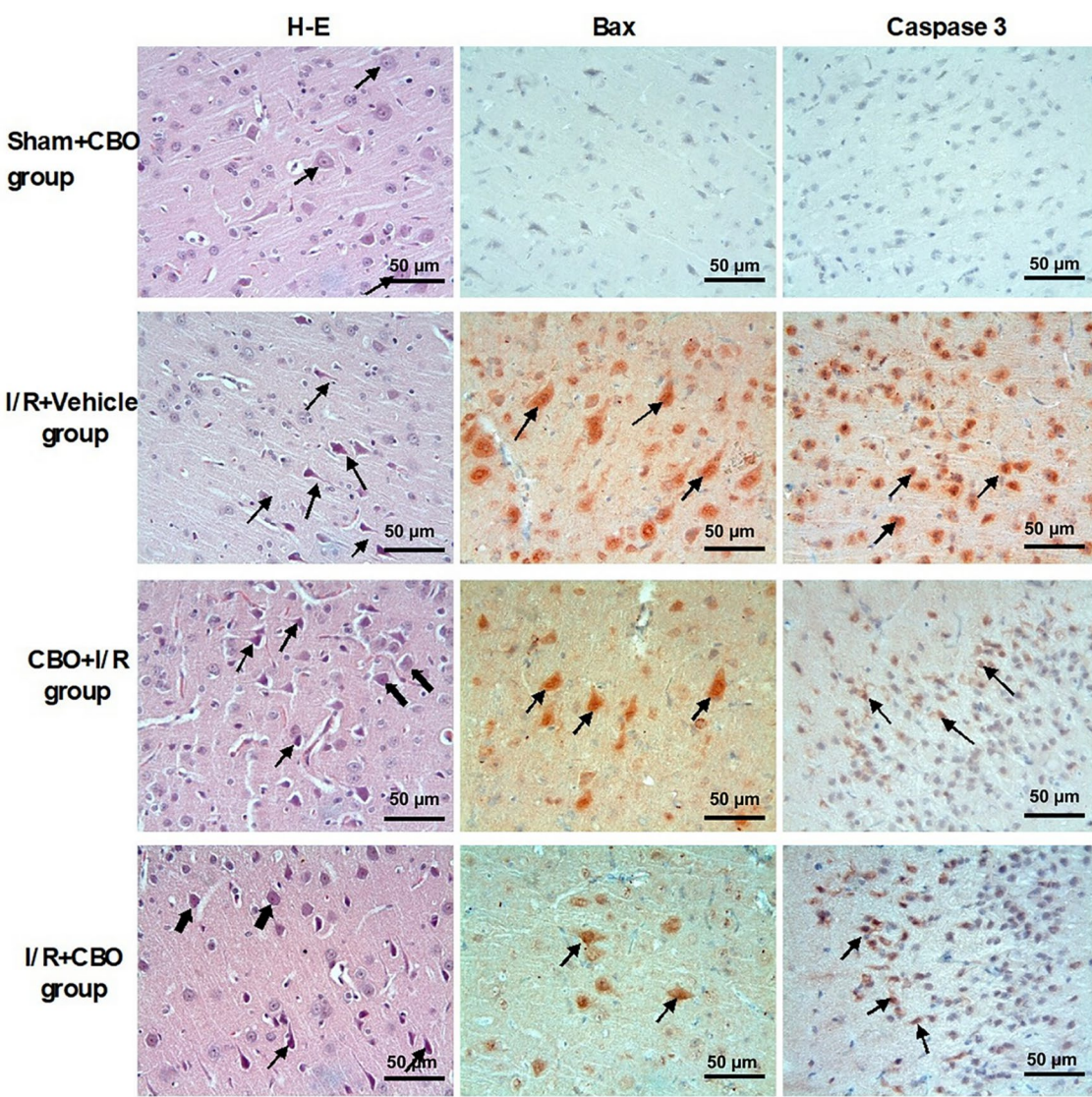


Fig. 4. Immunohistochemical appearance of the cortex. H-E: Sham + CBO group: Pyramidal neurons (arrows), recognizable by their large triangular bodies among the neurons. I/R + Vehicle group: Appearance of degenerated neurons with irregular borders, acidophilic cytoplasm, heterochromatic nuclei and shrunken nuclei (arrows). I/R + CBO group and CBO + I/R group: The appearance of decayed neurons among intact neurons (arrows). H-E: X400. Bax: Monitoring bax (+) cells in the cortex (arrows), X400. Caspase 3: Monitoring caspase-3 (+) cells in the cortex (arrows), CBO: Cinnamon Bark Oil; I/R: Ischemia–Reperfusion.

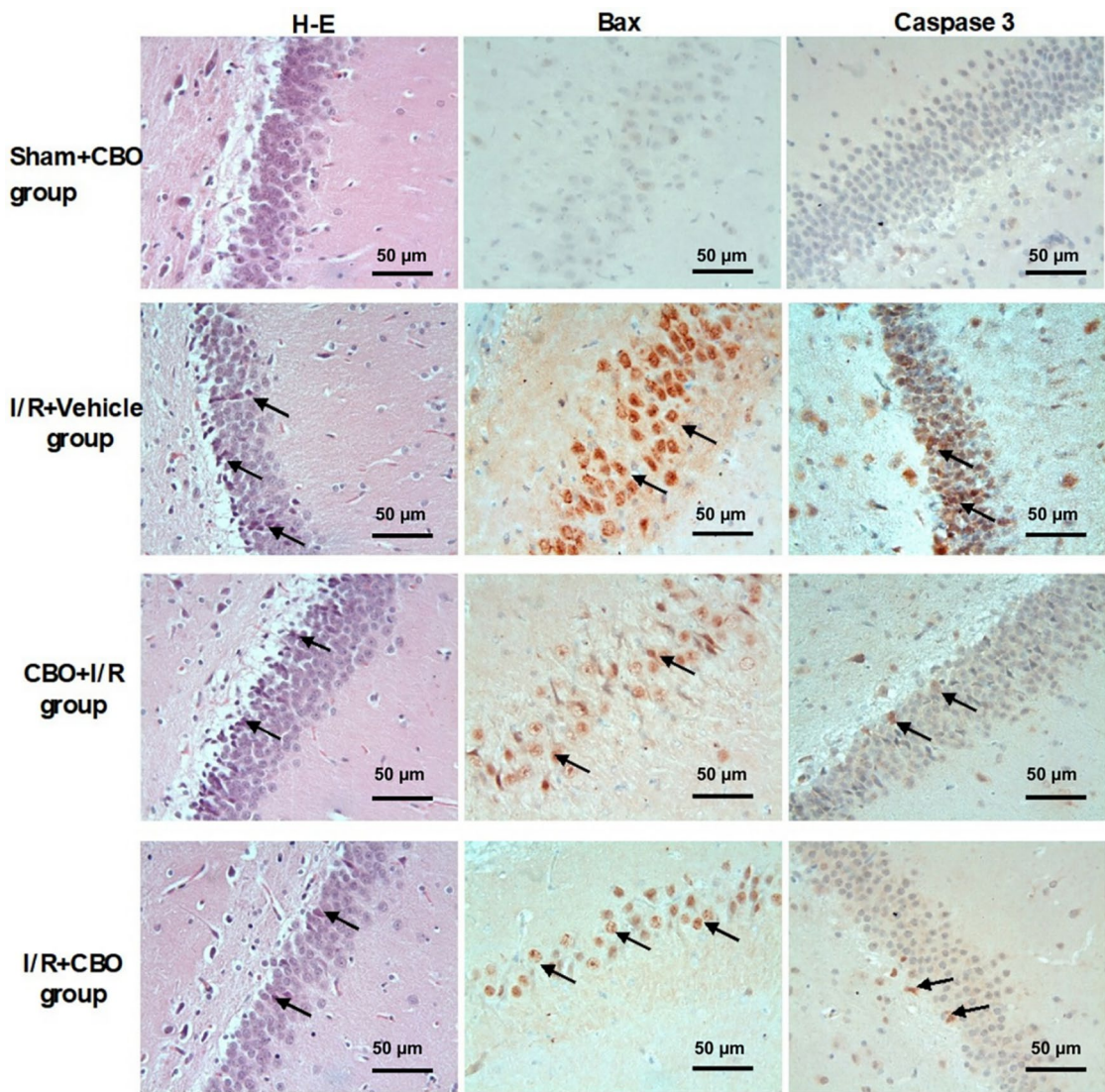


Fig. 5. Immunohistochemical appearance of the hippocampus. H-E; Sham + CBO group: Pyramidal neurons (arrows) recognized by their large triangular-shaped bodies among the neurons. I/R + Vehicle group: Appearance of degenerated neurons with irregular borders, acidophilic cytoplasm, heterochromatic nuclei and shrunken nuclei (arrows). I/R + CBO group and CBO + I/R group: Appearance of degenerating neurons among intact neurons (arrows). H-E: X400. Bax: Bax (+) cells are observed in the hippocampus (arrows), X400. Caspase 3: Caspase-3 (+) cells are observed in the hippocampus (arrows), X400 CBO: Cinnamon Bark Oil; I/R: Ischemia–Reperfusion.

Parameters	Sham + CBO Group (n:8)	I/R + Vehicle Group (n:8)	CBO + I/R Group (n:8)	I/R + CBO Group (n:8)
Number of degenerating neurons (cortex)	0.14 ± 0.35	6.24 ± 0.22 ^a	2.61 ± 1.56 ^b	3.84 ± 1.66 ^{b,c}
Number of degenerating neurons (hippocampus)	0.00 ± 0.00	6.28 ± 2.45 ^a	1.70 ± 1.60 ^b	2.21 ± 1.16 ^{b,c}
Number of Caspase 3 (+) cells (cortex)	0.17 ± 0.37	7.04 ± 2.04 ^a	1.38 ± 1.27 ^b	2.98 ± 2.17 ^{b,c}
Caspase 3 (+) cell count (hippocampus)	0.11 ± 0.32	3.60 ± 1.33 ^a	1.04 ± 0.76 ^b	3.40 ± 1.71 ^c
Number of Bax (+) cells (cortex)	0.20 ± 0.40	9.67 ± 2.95 ^a	6.90 ± 2.87 ^b	7.30 ± 1.85 ^b
Number of Bax (+) cells (hippocampus)	0.04 ± 0.20	11.95 ± 3.75 ^a	9.42 ± 1.62 ^b	10.15 ± 2.95 ^b

Table 4. Comparison of histopathologic findings. ^aStatistically significant difference with Sham + CBO ($p < 0.0001$). ^bStatistically significant difference with I/R + Vehicle ($p < 0.0001$). ^cStatistically significant difference with CBO + I/R ($p < 0.0001$). CBO, Cinnamon Bark Oil; I/R, Ischemia–Reperfusion.

The number of caspase-3 (+) cells was 2.98 ± 2.17 in the cortex and 3.40 ± 1.71 in the hippocampus in the sections where caspase-3 staining method was applied. When compared with the I/R + Vehicle group, the number of positive cells in this group was significantly decreased in the cortex ($p < 0.0001$), whereas there was no significant difference in the hippocampus. When compared with the I/R + CBO group, the number of positive cells was statistically significantly increased in this group ($p < 0.0001$).

The number of Bax (+) cells was found to be 7.30 ± 1.85 in the cortex and 10.15 ± 2.95 in the hippocampus. When compared with the I/R + Vehicle group, the number of positive cells in this group was statistically significantly decreased ($p < 0.0001$). When compared with the I/R + CBO group, there was no statistically significant difference between the groups ($p < 0.0001$) (Table 4).

Therapeutic (I/R + CBO) group: In H&E stained sections, the number of degenerated neurons was 2.61 ± 1.56 in the cortex and 1.70 ± 1.60 in the hippocampus in this group. Compared to the I/R + Vehicle group, the number of degenerated neurons in the cortex and hippocampus regions was significantly decreased ($p < 0.0001$).

The number of caspase-3 (+) cells was 1.38 ± 1.27 in the cortex and 3.60 ± 1.33 in the hippocampus in the sections where caspase-3 staining method was applied. A statistically significant decrease in the number of positive cells was observed in this group compared to the I/R + Vehicle group ($p < 0.0001$).

The number of Bax (+) cells was found to be 6.90 ± 2.87 in the cortex and 9.47 ± 1.62 in the hippocampus. A statistically significant decrease in the number of positive cells was observed in this group compared to the I/R + Vehicle group ($p < 0.0001$) (Table 4).

Discussion

Cerebral I/R injury is a clinical picture of progressive brain cell injury caused by I/R after cerebral ischemia. In the course of I/R process, necrosis and apoptosis may occur during neuronal. Although the reason for I/R injury is not fully explained, there are many different pathological mechanisms. In biochemical events activated by cerebral I/R injury, loss of tissue energy supply occurs firstly, and consequently, endothelial dysfunction and neutrophil sequestration are followed by ROS formation^{30,31}. Therefore, any factor that suppresses these formations can be applied for the treatment of cerebral ischemia. Cerebral I/R injury studies have been performed previously with bilateral CCAs occlusion modeling, but there is still no treatment that completely eliminates this injury.

Cinnamon extract significantly reduced OS markers and improved antioxidant enzyme activities in rats exposed to toxic agents. For example, cinnamon extract protected against cobalt-induced oxidative and inflammatory damage in heart, kidney, and liver tissues by suppressing oxidants and increasing antioxidants³². Cinnamon nanoemulsions mitigated pesticide-induced liver and kidney toxicity by upregulating antioxidant enzymes (SOD, GSH peroxidase, CAT) and reducing OS markers (MDA, H_2O_2)³³. Cinnamon bark extract lowered blood MDA levels in hyperglycemic rats, with the most pronounced effect at 100 mg/kg dosage³⁴. Cinnamon oil reduced kidney cell damage in diabetic rats, attributed to its polyphenol and flavonoid content with antioxidant activity³⁵.

This study provides robust experimental evidence that CBO, derived from *C. verum*, exerts significant neuroprotective effects against cerebral I/R injury in a rat model of bilateral CCAs occlusion. The protective mechanisms are multi-faceted, involving the potent attenuation of OS, modulation of inflammatory responses, and suppression of neuronal apoptosis. Crucially, these beneficial effects were demonstrated not only when CBO was administered prophylactically prior to ischemia but also when given therapeutically after reperfusion, highlighting its potential for both preventive and post-injury clinical applications.

Bilateral CCAs occlusion in rats is widely used to model global cerebral ischemia, but the resulting brain injury is often mild, variable, and primarily affects specific brain regions such as the hippocampus and white matter, rather than the motor cortex or basal ganglia, which are critical for motor coordination assessed by rotarod and accelerod tests^{17,36,37}. The degree of ischemia and resulting deficits can vary significantly depending on rat strain, age, and surgical technique, leading to inconsistent behavioral outcomes. Additionally, the presence of collateral blood flow (e.g., via the posterior communicating arteries) can further reduce the severity of ischemia, limiting observable motor deficits^{17,36}. The rotarod and accelerod tests are designed to detect gross motor coordination and balance deficits. However, bilateral CCAs occlusion-induced ischemia in rats often does not produce substantial motor impairment detectable by these tests, especially in chronic models, because the injury is not severe or widespread enough to disrupt the neural circuits required for these tasks. Studies have shown that while cognitive and sensory deficits are common after bilateral CCAs occlusion, significant motor deficits are less reliably observed unless the ischemic insult is more severe or involves additional brain regions^{17,37,38}. In line with this, no statistically significant differences were observed between the groups in our study, which employed bilateral carotid artery occlusion as the ischemia model.

The biochemical data consistently demonstrate that CBO effectively mitigates I/R-induced OS. The highest level of MDA, a well-established marker of lipid peroxidation resulting from ROS attack on cell membranes, was observed in the I/R group, confirming severe oxidative damage. Both prophylactic and therapeutic CBO administration markedly reduced MDA levels, with the therapeutic group showing the most pronounced decrease. This finding aligns with previous studies demonstrating that cinnamon extracts and their bioactive components, particularly cinnamaldehyde, reduce MDA in models of liver, kidney, cardiac, and brain toxicity induced by toxins or metabolic stress^{32,34,35}. Concurrently, CBO enhanced antioxidant defenses: SOD activity was significantly higher in the prophylactic group than in the I/R + Vehicle group, indicating an increased capacity to scavenge superoxide radicals. While tGSH levels were paradoxically lower in both CBO-treated groups compared to the Sham + CBO group, this likely reflects the consumption of GSH during active detoxification of ROS following I/R injury, a process CBO may facilitate rather than prevent entirely. More importantly, TAC was significantly increased in the prophylactic group and maintained at a higher level in the therapeutic group compared to the I/R + Vehicle group, suggesting CBO enhances the overall endogenous antioxidant network. The reduction in OSI in the CBO-treated groups further corroborates a net shift toward a less oxidized cellular

state. These results support the established antioxidant properties of cinnamon's phenolic compounds, including cinnamaldehyde and eugenol, which can donate hydrogen atoms to stabilize free radicals and inhibit lipid peroxidation cascades^{39,40}. The mechanism may involve the activation of the nuclear factor erythroid 2-related factor 2 (Nrf2) pathway, the master regulator of cellular antioxidant defense, leading to the upregulation of enzymes like heme oxygenase-1 (HO-1) and glutathione-S-transferase, as shown by cinnamaldehyde in other models⁴¹.

Regarding inflammation, CBO demonstrated a targeted and complex effect. While MPO activity was unexpectedly higher in the prophylactic group compared to the I/R + Vehicle group, this likely represents a complex, biphasic response. Increased SOD activity in the CBO + I/R group could lead to elevated H₂O₂ production, which serves as a substrate for MPO, potentially amplifying its activity transiently despite an overall anti-inflammatory outcome⁴². Importantly, however, CBO significantly suppressed the pro-inflammatory cytokine TNF- α in both treatment protocols compared to the I/R + Vehicle group. TNF- α is a central mediator of neuroinflammation in I/R injury, promoting leukocyte adhesion, microglial activation, and direct neuronal toxicity⁴. The suppression of TNF- α by CBO is consistent with prior research showing that *trans*-cinnamaldehyde inhibits the nuclear factor-kappa B (NF- κ B) signaling pathway, a master regulator of TNF- α and other inflammatory mediators like inducible nitric oxide synthase (iNOS) and cyclooxygenase-2 (COX-2)^{11,43}. Notably, IL-1 levels showed no significant differences across groups. This may reflect the temporal dynamics of cytokine release; IL-1 β typically peaks within hours after ischemia and declines during prolonged reperfusion periods like the 72-h window used here⁴⁴, suggesting our sampling time point may have missed its peak expression. The lack of change in IL-1 does not negate CBO's anti-inflammatory potential but underscores the need for future studies employing multiple time-point analyses to fully characterize its impact on the cytokine cascade. The paradoxical increase in MPO in the prophylactic group warrants further investigation into whether CBO alters neutrophil recruitment kinetics or activates specific enzymatic pathways downstream of ROS generation.

The most compelling evidence for CBO's neuroprotection lies in its potent anti-apoptotic effects, confirmed by both biochemical and histopathological analyses. Apoptosis, a major contributor to delayed neuronal death after I/R, is driven by mitochondrial dysfunction and the activation of caspase-dependent pathways. Our IHC analysis revealed a dramatic increase in the number of Bax-positive and caspase-3-positive cells in the cerebral cortex and hippocampus of I/R rats. Both prophylactic and therapeutic CBO treatments significantly reduced the density of these apoptotic markers in both brain regions. This finding is mechanistically supported by studies showing that sodium benzoate, a metabolite of cinnamaldehyde, reduces cytochrome c release and the Bax/Bcl-2 ratio in global ischemia models⁴⁵. Furthermore, *trans*-cinnamaldehyde has been shown to activate the phosphatidylinositol 3-kinase (PI3K)/protein kinase B (Akt) survival pathway and improve mitochondrial membrane potential, thereby inhibiting the intrinsic apoptotic cascade⁴⁶. The preservation of neuronal architecture in H&E-stained sections, with significantly fewer degenerated neurons exhibiting acidophilic cytoplasm and shrunken nuclei in the CBO-treated groups, provides direct morphological confirmation of this anti-apoptotic efficacy. The comparable effectiveness of prophylactic and therapeutic administration suggests CBO can intervene effectively even after the ischemic insult has occurred, a critical finding for clinical translation where treatment is almost always initiated post-event.

Our findings are consistent with a growing body of literature on *C. verum*. CBO's primary constituent, *trans*-cinnamaldehyde, has been repeatedly identified as the key bioactive agent responsible for its antioxidant, anti-inflammatory, and anti-apoptotic properties^{7,11}. It has been shown to activate the Nrf2 pathway, the master regulator of cellular antioxidant defense, leading to the upregulation of enzymes like HO-1 and glutathione-S-transferase⁴¹. Other constituents, such as eugenol and linalool, contribute synergistically by inhibiting peroxynitrite-induced nitrosative stress^{5,15}. The use of *C. verum* in this study is particularly significant due to its high cinnamaldehyde content (55–75%) and low coumarin levels (<0.5%), making it safer for chronic or repeated dosing compared to *C. cassia*¹⁶. This choice enhances the translational relevance of our findings, as *C. verum* is the authentic "true cinnamon" standardized by the European Pharmacopoeia and frequently used in experimental models investigating OS and inflammation²⁰.

Several limitations of this study warrant consideration. First, the exclusive use of female *Wistar albino* rats without monitoring estrous cycle phase represents a notable gap. Hormonal fluctuations can profoundly influence OS, inflammation, and apoptosis pathways, potentially confounding results⁴⁷. Future studies must include both sexes and account for hormonal status. Second, while sunflower oil was used as a vehicle, a dedicated I/R + Vehicle group would have better isolated any potential baseline effects of the solvent. Third, we did not measure the key anti-apoptotic protein Bcl-2; quantifying the Bax/Bcl-2 ratio would have provided a more complete picture of the apoptotic balance. Fourth, histopathological analysis was confined to the cortex and hippocampus, omitting the striatum—a region highly vulnerable to global ischemia due to its vascular supply. Including the striatum would offer a more comprehensive assessment of neuroprotection. Fifth, the observed increase in MPO activity in the prophylactic group, while statistically significant, requires further mechanistic investigation to determine if it represents a transient, hormetic response or an unintended consequence of enhanced SOD activity. Finally, while oral administration is clinically relevant, future work should investigate pharmacokinetics and optimal dosing regimens for CBO.

Conclusion

In summary, CBO significantly attenuated OS by reducing MDA levels and restoring antioxidant enzyme activities (SOD and CAT) in rats subjected to cerebral I/R. CBO also decreased inflammatory responses, as evidenced by reductions in MPO and IL-1 β , and modulated apoptotic pathways by lowering Bax and caspase-3 expression. Histopathological and IHC analyses further confirmed that CBO preserved neuronal structure in the cortex and hippocampus. These findings suggest that CBO exerts neuroprotective effects through combined antioxidant, anti-inflammatory, and anti-apoptotic mechanisms. Further studies including both sexes, additional brain

regions such as the striatum, and direct measurement of anti-apoptotic proteins are warranted to strengthen the translational potential of these results.

Data availability

The datasets generated and/or analyzed during the current study are included in the doctoral thesis of Melike Aba, deposited in the Council of Higher Education Thesis Center (<https://tez.yok.gov.tr/UlusTezMerkezi/giris.jsp>). The main text of the thesis is in Turkish; however, the relevant data will be made available in English upon reasonable request. Please contact Assoc. Prof. Onural Ozhan (onural.ozhan@inonu.edu.tr) for access.

Received: 7 August 2025; Accepted: 6 October 2025

Published online: 12 November 2025

References

1. Kuriakose, D. & Xiao, Z. Pathophysiology and treatment of stroke: present status and future perspectives. *Int. J. Mol. Sci.* **21**(20), 7609 (2020).
2. Powers, W. J. et al. Guidelines for the early management of patients with acute ischemic stroke: 2019 update to the 2018 guidelines for the early management of acute ischemic stroke: A guideline for healthcare professionals from the American heart association/american stroke association. *Stroke* **50**(12), e344–e418 (2019).
3. Mandalaneni, K., Rayi, A. & Jillella, D. V. Stroke reperfusion injury. StatPearls. Treasure Island (FL) ineligible companies. Disclosure: Appaji Rayi declares no relevant financial relationships with ineligible companies. Disclosure: Dinesh Jillella declares no relevant financial relationships with ineligible companies.: StatPearls Publishing Copyright © 2025, StatPearls Publishing LLC. (2025).
4. Yang, M., Liu, B., Chen, B., Shen, Y. & Liu, G. Cerebral ischemia-reperfusion injury: mechanisms and promising therapies. *Front. Pharmacol.* **16**, 1613464 (2025).
5. Xu, H., Lu, X., Qin, R., Shao, L. & Chen, L. the evolution of ischemia-reperfusion injury research in ischemic stroke: insights from a two-decade bibliometric analysis. *Brain Behav.* **15**(4), e70445 (2025).
6. Sabbaghzian, F., Soleimani, P., Eynshikh, F. R., Zafari, F. & Aali, E. Reduced ischemia-reperfusion oxidative stress injury by melatonin and N-acetylcysteine in the male rat brain. *IBRO Neurosci. Rep.* **17**, 131–137 (2024).
7. Singh, N. et al. Phytochemical and pharmacological review of Cinnamomum verum J. Presl-a versatile spice used in food and nutrition. *Food Chem.* **338**, 127773 (2021).
8. Ramazani, E. et al. Protective effects of cinnamomum verum, cinnamomum cassia and cinnamaldehyde against 6-OHDA-induced apoptosis in PC12 cells. *Mol. Biol. Rep.* **47**(4), 2437–2445 (2020).
9. Zhu, C. et al. Impact of Cinnamon Supplementation on cardiometabolic biomarkers of inflammation and oxidative stress: A systematic review and meta-analysis of randomized controlled trials. *Complement. Ther. Med.* **53**, 102517 (2020).
10. Commission, E. P. Medicines EDfTQo, Healthcare. European pharmacopoeia: Council of Europe (2013).
11. Chen, Y. F. et al. Trans-cinnamaldehyde, an essential oil in cinnamon powder, ameliorates cerebral ischemia-induced brain injury via inhibition of neuroinflammation through attenuation of iNOS, COX-2 expression and NF- κ B signaling pathway. *NeuroMol. Med.* **18**(3), 322–333 (2016).
12. Phytotherapy ESCo. E/S/C/O/P monographs: the scientific foundation for herbal medicinal products: Thieme (2003).
13. Singh, G., Maurya, S., DeLampasona, M. P. & Catalan, C. A. A comparison of chemical, antioxidant and antimicrobial studies of cinnamon leaf and bark volatile oils, oleoresins and their constituents. *Food Chem. Toxicol. Int. J. Publ. Br. Ind. Biol. Res. Assoc.* **45**(9), 1650–1661 (2007).
14. Chericoni, S., Prieto, J. M., Iacopini, P., Cioni, P. & Morelli, I. In vitro activity of the essential oil of Cinnamomum zeylanicum and eugenol in peroxynitrite-induced oxidative processes. *J. Agric. Food Chem.* **53**(12), 4762–4765 (2005).
15. McGrath, J. C., Drummond, G. B., McLachlan, E. M., Kilkenney, C. & Wainwright, C. L. Guidelines for reporting experiments involving animals: the ARRIVE guidelines. *Br. J. Pharmacol.* **160**(7), 1573–1576 (2010).
16. Abrahám, H. & Lázár, G. Early microglial reaction following mild forebrain ischemia induced by common carotid artery occlusion in rats. *Brain Res.* **862**(1–2), 63–73 (2000).
17. Handayani, E. S., Susilowati, R., Setyopranoto, I. & Partadiredja, G. Transient bilateral common carotid artery occlusion (tBCCAO) of rats as a model of global cerebral ischemia. *Bangladesh J. Med. Sci.* **18**(3), 491–500 (2019).
18. Ozhan, O. et al. Therapeutic effects of cinnamon bark oil on sciatic nerve injury in rats. *Eur. Rev. Med. Pharmacol. Sci.* **27**(12), 5841–5853 (2023).
19. Rana, P. & Sheu, S. C. Discrimination of four Cinnamomum species by proximate, antioxidant, and chemical profiling: towards quality assessment and authenticity. *J. Food Sci. Technol.* **60**(10), 2639–2648 (2023).
20. Kim, N. Y. et al. Cinnamomum verum extract inhibits NOX2/ROS and PKC δ /JNK/AP-1/NF- κ B pathway-mediated inflammatory response in PMA-stimulated THP-1 monocytes. *Phytomed. Int. J. Phytother. Phytopharmacol.* **112**, 154685 (2023).
21. Padmanabhan, A. M. & Doss, V. A. Combinatorial protective effect of Cinnamomum verum and Stingless Bee Honey against oxidative stress in isoproterenol-induced cardiotoxicity in Wistar rats. *Clin. Phytosc.* **11**(1), 3 (2025).
22. Bradford, M. M. A rapid and sensitive method for the quantitation of microgram quantities of protein utilizing the principle of protein-dye binding. *Anal. Biochem.* **72**, 248–254 (1976).
23. McCord, J. M. & Fridovich, I. Superoxide dismutase. An enzymic function for erythrocuprein (hemocuprein). *J. Biol. Chem.* **244**(22), 6049–6055 (1969).
24. Akerboom, T. P. & Sies, H. Assay of glutathione, glutathione disulfide, and glutathione mixed disulfides in biological samples. *Methods Enzymol.* **77**, 373–382 (1981).
25. Placer, Z., Veselkova, A. & Rath, R. Kinetics of malonyldialdehyde in the organism. *Experientia* **21**, 19–20 (1965).
26. Pulli, B. et al. Measuring myeloperoxidase activity in biological samples. *PLoS ONE* **8**(7), e67976 (2013).
27. Erel, O. A novel automated method to measure total antioxidant response against potent free radical reactions. *Clin. Biochem.* **37**(2), 112–119 (2004).
28. Erel, O. A novel automated direct measurement method for total antioxidant capacity using a new generation, more stable ABTS radical cation. *Clin. Biochem.* **37**(4), 277–285 (2004).
29. Erel, O. A new automated colorimetric method for measuring total oxidant status. *Clin. Biochem.* **38**(12), 1103–1111 (2005).
30. Bulkley, G. B. Reactive oxygen metabolites and reperfusion injury: aberrant triggering of reticuloendothelial function. *Lancet (London, England)*, 344(8927), 934–936 (1994).
31. Pattwell, D., McArdle, A., Griffiths, R. D. & Jackson, M. J. Measurement of free radical production by in vivo microdialysis during ischemia/reperfusion injury to skeletal muscle. *Free Radical Biol. Med.* **30**(9), 979–985 (2001).
32. Isik, B. et al. Protective effect of cinnamon extract against cobalt-induced multiple organ damage in rats. *Front. Pharmacol.* **15**, 1384181 (2024).
33. Aioub, A. A. et al. Cinnamon nanoemulsion mitigates acetamiprid-induced hepatic and renal toxicity in rats: biochemical, histopathological, immunohistochemical, and molecular docking analysis. *BMC Vet. Res.* **20**(1), 256 (2024).

34. Perisnawati, P., Yerizel, E. & Alimudin, T. The Effect of cinnamon bark extract (*Cinnamomum burmanii*) on blood Malondialdehyde (MDA) levels in Hyperglycemia rats. *Int. J. Res. Rev.* **11**(5), 1–6 (2024).
35. Budiastuti, B. et al. Effect of cinnamon oil (*Cinnamomum burmannii*) on the histological kidney of male diabetic rats (*Rattus norvegicus*). *Open Vet. J.* **15**(2), 923–930 (2025).
36. León-Moreno, L. C., Castañeda-Arellano, R., Rivas-Carrillo, J. D. & Dueñas-Jiménez, S. H. Challenges and improvements of developing an ischemia mouse model through bilateral common carotid artery occlusion. *J. Stroke Cerebrovasc. Dis.* **29**(5), 104773 (2020).
37. Li, H. et al. Comparison of bilateral carotid artery occlusion and stenosis in inducing behaviour and structural changes in rodents. *J. Biomed. Nanotechnol.* **19**(7), 1225–1238 (2023).
38. Kurkin, D. et al. Neuroprotective action of cortexin, cerebrolysin and actovegin in acute or chronic brain ischemia in rats. *PLoS ONE* **16**(7), e0254493 (2021).
39. Gulcin, I. et al. Anticholinergic, antidiabetic and antioxidant activities of cinnamon (*cinnamomum verum*) bark extracts: polyphenol contents analysis by LC-MS/MS. *Int. J. Food Prop.* **22**(1), 1511–1526 (2019).
40. Ranasinghe, P. et al. Medicinal properties of 'true' cinnamon (*Cinnamomum zeylanicum*): a systematic review. *BMC Complement. Altern. Med.* **13**, 275 (2013).
41. Long, M. et al. Nrf2-dependent suppression of azoxymethane/dextran sulfate sodium-induced colon carcinogenesis by the cinnamon-derived dietary factor cinnamaldehyde. *Cancer Prev. Res.* **8**(5), 444–454 (2015).
42. Chen, S., Chen, H., Du, Q. & Shen, J. Targeting Myeloperoxidase (MPO) Mediated Oxidative Stress and Inflammation for Reducing Brain Ischemia Injury: Potential Application of Natural Compounds. *Front. Physiol.* **11**, 433 (2020).
43. Schink, A. et al. Anti-inflammatory effects of cinnamon extract and identification of active compounds influencing the TLR2 and TLR4 signaling pathways. *Food Funct.* **9**(11), 5950–5964 (2018).
44. Armogida, M., Nisticò, R. & Mercuri, N. B. Therapeutic potential of targeting hydrogen peroxide metabolism in the treatment of brain ischaemia. *Br. J. Pharmacol.* **166**(4), 1211–1224 (2012).
45. Gao, Y. et al. Protective Effects of Sodium (±)-5-Bromo-2-(α-Hydroxypentyl) Benzoate in a Rodent Model of Global Cerebral Ischemia. *Front. Pharmacol.* **8**, 691 (2017).
46. Qi, X. et al. Trans-cinnamaldehyde protected PC12 cells against oxygen and glucose deprivation/reperfusion (OGD/R)-induced injury via anti-apoptosis and anti-oxidative stress. *Mol. Cell. Biochem.* **421**(1–2), 67–74 (2016).
47. Haast, R. A., Gustafson, D. R. & Kiliaan, A. J. Sex differences in stroke. *J. Cereb. Blood Flow Metab. Off. J. Int. Soc. Cereb. Blood Flow Metab.* **32**(12), 2100–2107 (2012).

Author contributions

Melike Aba: Conceptualization, Data curation, Writing, Reviewing, Editing. Yuksel Kablan: Supervision, Writing, Reviewing and Editing. Onural Ozhan: Establishing the experimental model. Elif Karaca: Histopathological analysis. Ahmet Ulu: Biochemical analysis. Burhan Ates: Biochemical analysis, Interpretation. Nigar Vardi: Histopathological analysis, Interpretation. Hakan Parlakpinar: Supervision, Interpretation, Reviewing and Editing.

Funding

This work was supported by Research Fund of the Inonu University. Project Number: TTU-2020-2147).

Declarations

Competing interests

The authors declare no competing interests.

Ethical approval and consent to participate

This experimental study obtained ethical approval (Protocol no: Ethical approval number: 2020/3-8) from the Experimental Animal Ethics Committee of Inonu University Faculty of Medicine.

Consent for publication

Not applicable.

Clinical trial number

Not applicable.

Additional information

Correspondence and requests for materials should be addressed to O.O.

Reprints and permissions information is available at www.nature.com/reprints.

Publisher's note Springer Nature remains neutral with regard to jurisdictional claims in published maps and institutional affiliations.

Open Access This article is licensed under a Creative Commons Attribution-NonCommercial-NoDerivatives 4.0 International License, which permits any non-commercial use, sharing, distribution and reproduction in any medium or format, as long as you give appropriate credit to the original author(s) and the source, provide a link to the Creative Commons licence, and indicate if you modified the licensed material. You do not have permission under this licence to share adapted material derived from this article or parts of it. The images or other third party material in this article are included in the article's Creative Commons licence, unless indicated otherwise in a credit line to the material. If material is not included in the article's Creative Commons licence and your intended use is not permitted by statutory regulation or exceeds the permitted use, you will need to obtain permission directly from the copyright holder. To view a copy of this licence, visit <http://creativecommons.org/licenses/by-nc-nd/4.0/>.

© The Author(s) 2025